Low-temperature magnetic anisotropy in micas and chlorite

Authors

Andrea R. Biedermann[1], Christian Bender Koch[2], Wolfram E.A. Lorenz[3], Ann M. Hirt[1,*]

[1] Institute of Geophysics, ETH Zurich, Sonneggstrasse 5, CH-8092 Zurich, Switzerland

[2] Department of Chemistry, University of Copenhagen, Universitetsparken 5, DK-2100 Copenhagen Ø, Denmark

[3] Laboratory of Solid State Physics, ETH Zurich, Schafmattstrasse 16, CH-8093 Zurich, Switzerland

The final version of this article can be downloaded from the Tectonophysics website, DOI: doi:10.1016/j.tecto.2014.01.015

Abstract

Phyllosilicates, such as micas and chlorite, are common rock-forming minerals and often show preferred orientation in deformed rocks. In combination with single-crystal anisotropy, this leads to anisotropy of physical properties in the rock, such as magnetic susceptibility. In order to effectively use the magnetic anisotropy to understand a rock fabric, it is necessary to identify the minerals responsible for the magnetic anisotropy. Techniques have been developed to separate contributions of the ferrimagnetic, antiferromagnetic, paramagnetic, and diamagnetic susceptibilities to the anisotropy of magnetic susceptibility. Because diamagnetic and paramagnetic susceptibility are both linearly dependent on field, separation of the anisotropic contributions requires understanding how the degree of anisotropy of the paramagnetic susceptibility changes as a function of temperature. Note that diamagnetic susceptibility is not dependent on temperature. The increase in paramagnetic anisotropy at low temperature is used to separate the paramagnetic and diamagnetic subfabrics, and can be expressed by the p_{77} factor. In this study, we determined p_{77}, which is the change in the degree of anisotropy (δk) between room temperature (298 K) and liquid nitrogen temperature (77 K), for a series of micas and chlorite. The paramagnetic susceptibility ellipsoid is highly oblate with the minimum principal susceptibility normal to the silicate layers at both 77 K and RT. The degree of anisotropy δk increases by a factor of approximately 6.3 – 8.7 for individual samples of muscovite, phlogopite and chlorite on cooling from RT to 77 K and between 11.2 – 12.4 for biotite. A decrease in temperature enhances the paramagnetic anisotropy in a mineral. Biotite exhibits a relative stronger enhancement due to the onset of magnetic ordering below ~100 K. This can have important implications for interpreting low temperature anisotropy in mudstones, mica schists and gneisses.

Keywords:

phyllosilicate

AMS (anisotropy of magnetic susceptibility)

biotite, chlorite, muscovite, phlogopite

p_{77}

Highlights:

> AMS is enhanced by a factor of approx. 7 to 12 at 77 K compared to room temperature

> p_{77} in biotite is larger than in muscovite, phlogopite and chlorite

> AMS ellipsoid is oblate both at 77 K and RT

1. Introduction

The anisotropy of magnetic susceptibility (AMS) of a rock depends on mineral content, degree of preferred mineral orientation, and intrinsic anisotropy of the individual minerals. Because of their sheet-like morphology, phyllosilicate minerals are strongly anisotropic and become preferentially aligned during the formation of some types of rocks and play an important role in rock deformation. The magnetic anisotropy factors and the intrinsic anisotropies of these minerals have been the topic of a series of investigations (Borradaile et al., 1987; Borradaile and Werner, 1994; Martín-Hernández and Hirt, 2003; Zapletal, 1990). These studies demonstrated the importance of separating the effects of ferromagnetic inclusions in the phyllosilicates from the paramagnetic component. It is essential to understand the magnetic anisotropy of single crystals when investigating the magnetic anisotropy in a rock. High-field methods have been successful in separating the ferrimagnetic contribution to the AMS from the non-ferrimagnetic components (e.g. Hrouda and Jelinek, 1990; Kelso et al., 2002; Martín-Hernández and Ferré, 2007; Martín-Hernández and Hirt, 2001, 2004). Other methodologies have been designed to enhance the contribution of specific magnetic components: for example, heating a rock can induce the formation of new ferromagnetic minerals that mimic the overall mineral fabric (Borradaile and Lagroix, 2000; Henry et al., 2007; Schultz-Krutisch and Heller, 1985; Urrutia-Fucugauchi and Tarling, 1983).

The paramagnetic susceptibility (χ) is temperature-dependent according to the Curie-Weiss law: $\chi = \frac{C}{T-\theta}$, where T is the temperature, θ the paramagnetic Curie temperature and C a material constant. Lowering the temperature can lead to an enhancement of the paramagnetic fabric in a rock. Several studies in the 1980s used low temperature methods to define the paramagnetic susceptibility in different lithologies dominated by phyllosilicates (Rochette et al., 1983; Rochette, 1987; Rochette and Fillion, 1988). Ihmlé et al. (1989) first

demonstrated this enhancement by measurements of low-field AMS (LF-AMS) on iron-rich carbonates. Other studies have since applied the method to other rock types (Debacker et al., 2009; Hirt et al., 2004; Lüneburg et al., 1999; Pares and van der Pluijm, 2002; Richter and van der Pluijm, 1994). It must be noted, however, that both the paramagnetic susceptibility and its anisotropy are temperature-dependent. Both *C* and θ show directional dependencies and consequently the degree of anisotropy does not scale linearly with temperature (e.g. Coey, 1988). This is especially the case at low temperatures, where the degree of anisotropy can be quite high (Ballet and Coey, 1982). With k_1 and k_3 denoting the maximum and minimum principal susceptibilities, respectively, Schmidt et al. (2007b) defined the factor p_{77} to describe the increase in the AMS at 77 K compared to room temperature (RT), as

$$p_{77} = \frac{\partial k(77\ K)}{\partial k(RT)} = \frac{k_1(77\ K) - k_3(77\ K)}{k_1(RT) - k_3(RT)}$$

They demonstrated how this factor could be used to separate the diamagnetic and paramagnetic subfabrics. In a systematic study of the AMS of carbonate minerals Schmidt et al. (2007a) showed that p_{77} changed with the cation composition of the carbonates.

Phyllosilicates can be divided into different groups based on the stacking of tetrahedral (T) and octahedral (O) layers (Figure 1). Micas, including biotite, phlogopite and muscovite, consist of sandwiches of TOT layers, which are negatively charged and ionically bonded by cations, such as K, Na or Ca between the adjacent TOT layers. The mica group can be further subdivided into dioctahedral and trioctahedral micas. In dioctahedral micas, e.g. muscovite, only two thirds of the octahedral sites are filled, whereas in trioctahedral micas the octahedral sheet is fully occupied by cations. Biotite and phlogopite belong to this latter group. Muscovite has the general composition $KAl_2AlSi_3O_{10}(OH)_2$ and phlogopite and biotite form a solid solution series with ideal composition $K(Mg,Fe)_3AlSi_3O_{10}(OH)_2$. Chlorite is another phyllosilicate that has an additional octahedral interlayer between the TOT sets, thus forming

a TOTO structure. Iron, which controls the magnetic properties of these minerals, is dominantly located in the octahedral sheets.

Several studies have examined the temperature dependent AMS in phyllosilicate minerals. Beausoleil et al. (1983) determined the paramagnetic Curie temperatures θ and Curie constants C for eight biotites, and found that the values of both θ and C varied depending on whether the field was applied parallel or perpendicular to the silicate sheets. Similar behaviour has been found for other phyllosilicates (Ballet and Coey, 1982; Ballet et al., 1985). Pares and van der Pluijm (2002) described a method to measure AMS at liquid nitrogen temperature (77 K) and showed a change in the degree of anisotropy $\frac{k_1}{k_3}$ for chlorite, muscovite and biotite. Biotite exhibited the strongest increase in $\frac{k_1}{k_3}$ – by approximately 1.8 – followed by muscovite and chlorite, which increased by a factor of 1.1. They then compared this to the increase observed in natural rocks, in an attempt to characterize which phyllosilicate controlled the observed AMS.

In this study we define the low-temperature anisotropy and p_{77} for a collection of phlogopite, biotite, muscovite and chlorite crystals so that these properties can be used in the isolation of diamagnetic from paramagnetic subfabrics. The results are used to evaluate the influence of chemical composition on the AMS.

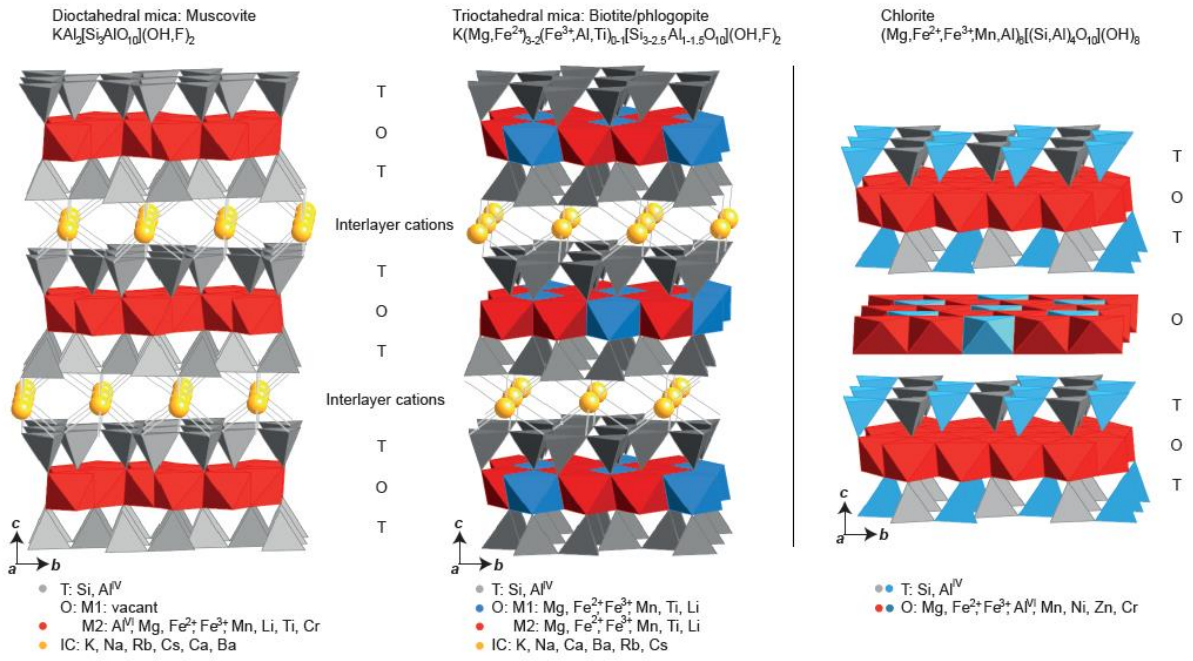

Figure 1: Crystal structures and typical site occupancies for di- and trioctahedral mica and chlorite. Mica has a TOT structure, whereas chlorite possesses a TOTO structure. Images were made with CrystalMaker.

2. Material and methods

2.1 Sample preparation

A total of 33 mineral samples, including five biotites, 18 phlogopites, five muscovites and five chlorites were analyzed (Table 1). The samples were obtained from several sources: (1) Ward's Natural Science Establishment, (2) the mineral collection of the Department of Earth Sciences, ETH-Zürich (cf. Martín-Hernández and Hirt, 2003), and (3) some were collected during fieldwork at Oldoinyo Lengai in Tanzania. The sample collection in this study includes crystals used by Martín-Hernández and Hirt (2003) to characterize room-temperature anisotropy in these minerals. Samples were first cleaned in alcohol using an ultrasonic cleaner and then cut, weighed and fitted into plastic holders. The basal plane of each cuboid sample was oriented parallel to the sheet-like structure, within which the orientations of the crystallographic b-axes were unknown. In nature it is the silicate sheets that

show strong preferential orientation in deformed rocks, while the a- and b-axes are not aligned.

2.2 Chemical analysis and Mössbauer spectroscopy

Chemical composition of the single crystals was measured on a JEOL JXA-2800 electron microprobe at the Institute of Geochemistry and Petrology, ETH Zurich. Measurements were performed using an accelerating voltage of 15 kV, a beam current of 20 nA, and a focused beam. Synthetic and natural oxides were used as standards. Ten spots were measured per sample in order to check their homogeneity. If inclusions were visible, they were also analysed. Data were φ-ρ-z-corrected and reported as oxides. The electron microprobe allows for very accurate measurements of the major element composition. However, it cannot distinguish between ferric and ferrous iron. Thus, as a first approximation, we assumed that all iron is present as Fe^{2+}.

Selected samples were analysed by Mössbauer spectroscopy at room temperature using a conventional constant acceleration spectrometer. The spectrometer was calibrated using the spectrum of a thin foil of natural iron at room temperature and a thin flake of the sample was placed at the magic angle for measurement (approx. 0.5 cm^2 of sample). The spectra were fitted using doublet components with Lorentzian line shapes (one doublet for Fe^{2+} - two doublets for some muscovites - and one for Fe^{3+}) constraining the two lines of the doublets to be identical. Assuming identical f-factors for the components, the relative spectral area is identical to the relative occurrence. The presence of iron oxides was positively identified in the spectrum of chlorite Zer3 by the occurrence of magnetically ordered sextets (approximately 35 % of the spectral area). Fe^{2+}/Fe^{3+} ratios from the Mössbauer spectra were used together with the total Fe content from electron probe microanalysis (EPMA) to calculate the FeO and Fe_2O_3 contents.

In addition, we used several methods to try to map the Fe/Mg distribution in the octahedral sheets of phlogopite. In a first step, iron and magnesium contents were mapped on a sheet-parallel surface with the electron microprobe at a horizontal resolution of 1 μm. Further techniques used for elemental imaging were EELS/EFTEM at the Electron Microscopy Center of the ETH Zurich (EMEZ) and scanning transmission X-ray microspectroscopy (STXM) at the Swiss Light Source, Paul Scherrer Institut, Villigen, Switzerland. The latter measurements were obtained from the PolLux beamline with a spatial resolution of ca. 30-50 nm. Samples for both techniques were FIB (focused ion beam) sections of ca. 100 nm thickness prepared by the so-called H-bar technique at EMEZ.

2.3 Mean susceptibility and high-field magnetic anisotropy

Magnetic susceptibility is described mathematically by a second-order, symmetric tensor, which can be represented geometrically by an ellipsoid with principal axes $k_1 \geq k_2 \geq k_3$. The ellipsoid can be determined from measuring susceptibility along specified directions and in low or high magnetic fields. Mean susceptibility is defined as $k_{mean} = \frac{1}{3}(k_1 + k_2 + k_3)$ and was measured on an AGICO MFK1-FA susceptibility bridge in a 200 A/m field and frequency of 976 Hz. For samples with a high ferromagnetic content, the mean susceptibility of the silicate lattice was defined from the high-field slope of hysteresis loops. Hysteresis was measured on a Princeton Measurements Corporation MicroMag Vibrating Sample Magnetometer in magnetic fields up to 1 T.

The anisotropy of magnetic susceptibility was determined in high-fields on a torque magnetometer (Bergmüller et al., 1994) at the Laboratory for Natural Magnetism, ETH Zurich. Measurements were performed at 30° increments in three perpendicular planes, one being parallel and two perpendicular to the basal plane of the crystals. Six fields between 1.0 T and 1.5 T were applied. These fields are strong enough so that the ferrimagnetic

contribution to the anisotropy, arising from e.g. magnetite inclusions, is saturated. All measurements were made at room temperature and at 77 K. For the low temperature measurements a cryostat was fitted between the poles of the electromagnet, so that the sample was submersed in liquid nitrogen during the measurement (cf. Schmidt et al., 2007b). The sample holder added a small contribution to the measured torque signal both at room temperature and at 77 K. This was corrected for by measuring the empty sample holder and subtracting its signal from the data. Finally, the paramagnetic component of the anisotropy was isolated with the method outlined in Martín-Hernández and Hirt (2001). The paramagnetic susceptibility ellipsoids were then used to determine the increase of the degree of anisotropy at 77 K. The degree of the paramagnetic anisotropy can be defined as $\delta k = k_1 - k_3$ (Schmidt et al., 2007b). Alternatively it can be defined by the deviatoric susceptibility, *k'* (Jelinek, 1984), and the shape of the ellipsoid by $U = \frac{2k_2 - k_1 - k_3}{k_1 - k_3}$ (Jelinek, 1981). We use δk to define the degree of anisotropy similar to Schmidt et al. (2007a), who defined p_{77} for carbonate minerals, however, will also show that this is similar to k'_{77K}/k'_{RT}.

2.4 Low-temperature magnetization curves

For one sample of each mica (Mu301, Bio202, Phl101), low-temperature magnetic properties were measured on a QuantumDesign Magnetic Property Measurement System (MPMS) at the Laboratory for Solid State Physics, ETH Zurich. We performed two kinds of measurements: (1) field-dependence of the magnetization at a given temperature (2 K, 25 K, 77 K or 300 K) and (2) temperature-dependence of the magnetization in a set field (1 T or 0.01 T) upon cooling from room temperature to 2 K. Field-dependence was determined in applied fields ranging from 0 T to 7 T in 0.5 T or 1 T steps, depending on the temperature. For the temperature-curves, measurements were taken every 10 K between 300 K and 80 K, every 5 K between 75 K and 10 K and with 1 K steps down to 2 K and temperatures were stabilized

for each data point. Small chips of the samples were mounted inside plastic straws so that the applied magnetic field was either parallel or perpendicular to their basal plane.

Susceptibility obtained from these measurements was fitted with a Curie-Weiss law:

$$\chi_{obs} = \frac{M}{H} = \mu_0 \frac{C}{T - \theta} + \chi_0$$

where χ_{obs} is the observed susceptibility, *M* the measured magnetization in the applied field *H*, θ the ordering temperature, *T* the observation temperature, μ_0 the permeability of free space, C the Curie constant and χ_0 is a temperature-independent background, i.e. diamagnetic or van Vleck susceptibility. The latter is a paramagnetic susceptibility, which is however independent of temperature. The background correction will not be considered further, as it is only of importance for the fitting process. The Curie constant is defined as $C = \frac{{\mu_B}^2 g^2 S(S+1)N}{3k_b}$ with μ_B the Bohr magneton, g Landé's g-factor, k_b Boltzmann's constant, *N* the number of magnetic ions and *S* their spin. Ferrous iron possesses a spin of 2, and ferric iron S = 5/2. The Curie constant is anisotropic as the *g*-factors are anisotropic for Fe^{2+}. Whereas the 3d shell of Fe^{3+} is half-filled and its g-factor is equal to 2, Fe^{2+} contains six electrons in its 3d shell and its g-factors are > 2. Typically, g is not known and needs to be measured by electron spin resonance or from low-temperature magnetization curves. We determined the *g*-factors perpendicular to and within the basal plane based on magnetization curves.

If both θ and χ_0 are zero, the susceptibility scales linearly with inverse temperature and passes through the origin of the coordinate system. For a typical measurement, however, both values are nonzero. Even in the paramagnetic range, inverse susceptibility is not perfectly linear with temperature, which is due to the temperature-independent contributions to the magnetization. Additionally, a negative θ shifts the curve towards lower temperatures, whereas a positive θ results in a shift to higher temperatures.

3. Results

3.1 Chemical composition

Average chemical compositions for all samples are given in Table 2. The low spot-to-spot variability for most samples shows that the chemical composition of the crystals is homogeneous and that the analysis is representative for the bulk sample. Micas and chlorite contain significant amounts of anions, OH^-, Cl^- or F^-, which have not been measured in our analysis. Therefore, we expect a total of ca. 95 wt.% of cations for muscovite, biotite and phlogopite and between 85 wt.% and 90 wt.% for chlorite. Most of our analyses meet the expected total, however, Bio101, Bio104, PhlT8-9 and PhlT10-13 show lower values between 70 and 90 wt.%. This is most likely due to uneven surfaces – especially for Bio101 and Bio104 flakes broke out of the structure upon polishing. Assuming that the relative amounts of cations are correct, these analyses have been normalized to a total of 95 wt.%.

For our study of magnetic properties, the contents of iron, manganese and chromium are of main importance, as these cations have large magnetic moments and dominate the magnetic properties even when only small amounts are present. All samples contain only small amounts of Mn (< 1 wt.% MnO) and Cr (< 0.5 wt.% Cr_2O_3). The FeO content varies between 1.5 – 2.4 wt.% for muscovite, 1.6 – 8.2 wt.% for phlogopite, and 9 – 18 wt.% for biotite. It is less variable in chlorite and is approximately 4 wt.% in all crystals. The chlorite samples Nzer1, Nzer2 and Zer3 showed microscopically visible iron oxide inclusions.

Mössbauer spectra show that Fe^{2+} dominates over Fe^{3+} in all minerals. In muscovite the Fe^{2+}/Fe^{3+} ratio varies and Fe^{2+} makes up between 80 % and 100 % of the total iron. The biotites contain ca. 95% Fe^{2+}, whereas the chlorite crystals contain between 60% and 90% Fe^{2+} (Table 3). Figure 2 shows that the Mössbauer spectra of chlorite, biotite and phlogopite can be modelled with one doublet each of ferric and ferrous iron. Two Fe^{2+} doublets are necessary, however, to fit the spectrum of Mu201, due to differences in the local environment

of Fe^{2+}. This variation could be due to a change in the coordination caused by the influence of the next-nearest neighbours. The narrow Fe^{2+} doublets in biotite, phlogopite and chlorite show that in these minerals, only small variations occur in the local coordination of Fe^{2+}. The different behaviour of muscovite compared to phlogopite and biotite could be due to the different site occupancies in dioctahedral and trioctahedral micas. More work on muscovite would be needed to fully characterize these variations. The ferric components in all samples exhibit one doublet with two distinct peaks in the micas. For chlorite the peaks are rather close. This could be explained by a different geometry associated with the change from a TOT structure in micas to TOTO in chlorite.

STXM was carried out to examine the chemical variability in the octahedral sheets of phlogopite crystals on the nanometer scale. Phlogopite was chosen because some crystals from Notre-Dame-du-Laus in Canada (sample Phl101, and to a lesser extent Phl1B and Phl1C) displayed an anisotropy within the basal plane. In addition, one biotite sample (Bio501) was measured for comparison. Both Fe and Mg concentrations were mapped on several grids with minimum point spacing of 10 nm and appear to be homogeneously distributed. Further high-resolution TEM images of the phlogopite crystals were acquired at EMEZ. However, the Fe concentration in our sample was below the detection limit of the instrument.

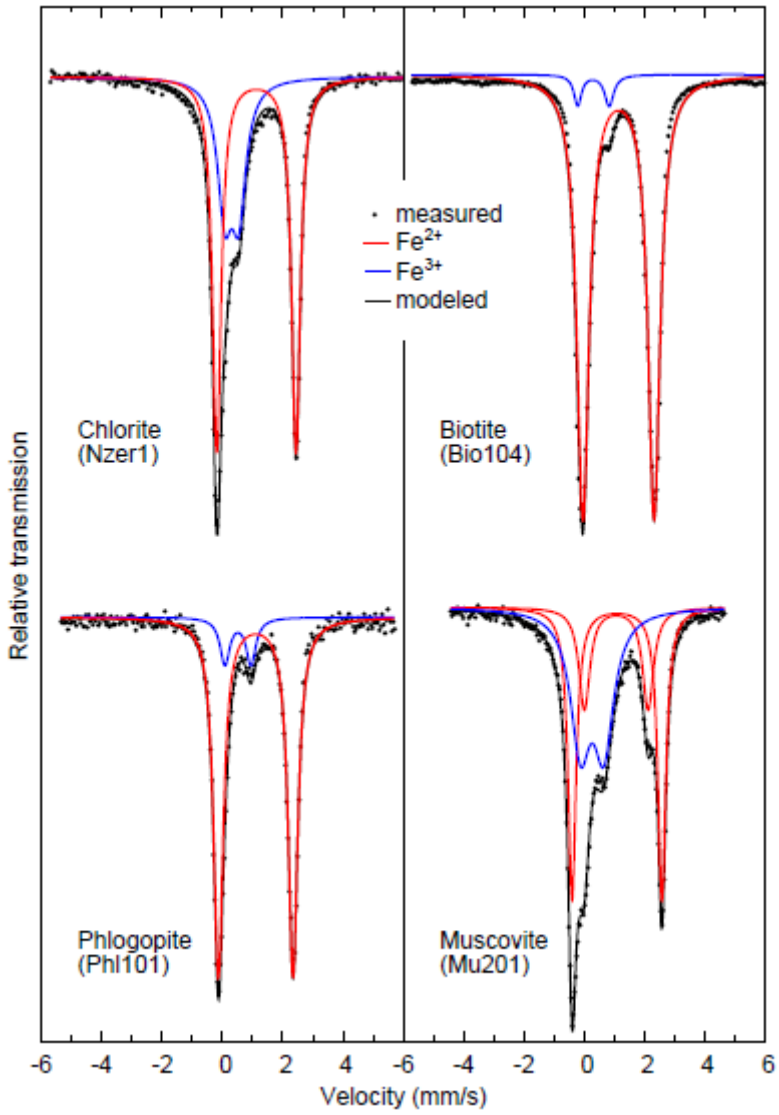

Figure 2: Measured and modelled Mössbauer spectra for one sample each of muscovite, biotite, phlogopite and chlorite (sample codes are given in the figure). Biotite, phlogopite and chlorite can be fitted with one ferric and one ferrous component. Muscovite needs two distinct doublets for the ferrous iron.

3.2 Mean susceptibility and high-field AMS

3.2.1 Mean susceptibility

Mean susceptibility ranges from $3.0*10^{-8}$ m^3/kg to $3.9*10^{-8}$ m^3/kg for muscovite and from $8.0*10^{-8}$ m^3/kg to $8.8*10^{-8}$ m^3/kg for chlorite. Biotite possesses higher susceptibility which varies between $3.4*10^{-7}$ m^3/kg and $3.8*10^{-7}$ m^3/kg. In phlogopites from Notre Dame-du-Laus, the susceptibility varies between $1.5*10^{-8}$ m^3/kg and $5.6*10^{-8}$ m^3/kg. For these samples, induced magnetization as a function of applied field demonstrated pure paramagnetic behaviour. Some samples from Oldoinyo Lengai had mean susceptibilities as high as $1.7*10^{-6}$ m^3/kg. The larger susceptibilities and high variability thereof in the latter group are related to ferromagnetic inclusions in these phlogopite crystals. For these samples, we used the high-field slope of magnetization curves to define the susceptibility (Table 1). Mean susceptibility shows an approximately linear increase with increasing iron content (Figure 3). The two biotite crystals whose chemical analyses only reached 70 – 73 wt.% lie above the linear trend.

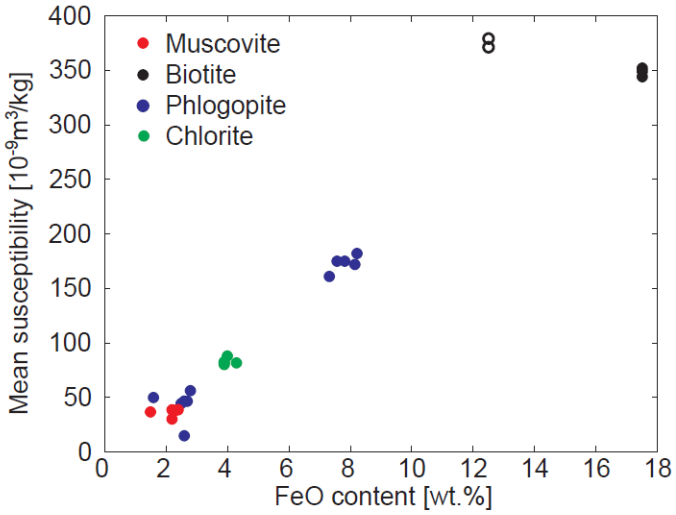

Figure 3:Mean susceptibility as a function of iron content for muscovite, biotite, phlogopite and chlorite. The mean susceptibility increases with increasing iron content. Bio101 and Bio104 shown with open circles had chemical analyses that only added up to a total of 70 and 73 wt.%, respectively.

3.2.2 High-field AMS: Micas

The high-field AMS of biotite, phlogopite and muscovite is dominated by the paramagnetic component at both room temperature and when measured at 77 K. All samples show a linear increase in the torque as a function of the square of the applied field (B^2) in all three planes with an intercept close to zero, which is expected for a purely paramagnetic mineral. The torque signal is, however, one to three orders of magnitude smaller when rotating within the basal plane of biotite, muscovite and most phlogopites (Figure 4). The torque signal increases by an order of magnitude at 77 K. The shape of the AMS ellipsoid of the paramagnetic fabric is highly oblate for most samples at both room temperature and 77 K, with k_3 normal to the basal plane, and k_1 and k_2 distributed within this basal plane (Figure 5, Table 4). Biotite, which incorporates the largest amount of iron in its structure, generates a stronger torque response than muscovite.

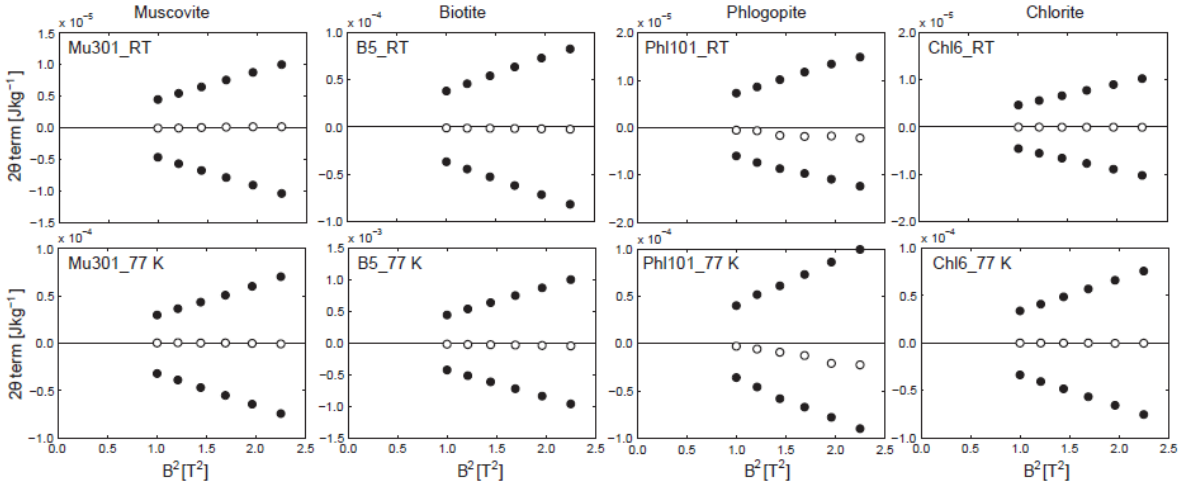

Figure 4: 2ϑ-component of the torque signal as a function of B^2 at room temperature and 77 K. Different subsets of data are shown for each of the three measurement planes. The linear relationship is typical for a paramagnetic material. In muscovite, biotite and chlorite, the torque signal is orders of magnitude smaller in the basal plane (open symbols) than in the other two measurement planes that are orthogonal to the basal plane (filled symbols). Phlogopite Phl101, however, shows a significant anisotropy in the basal plane. Note the different scales on the vertical axes.

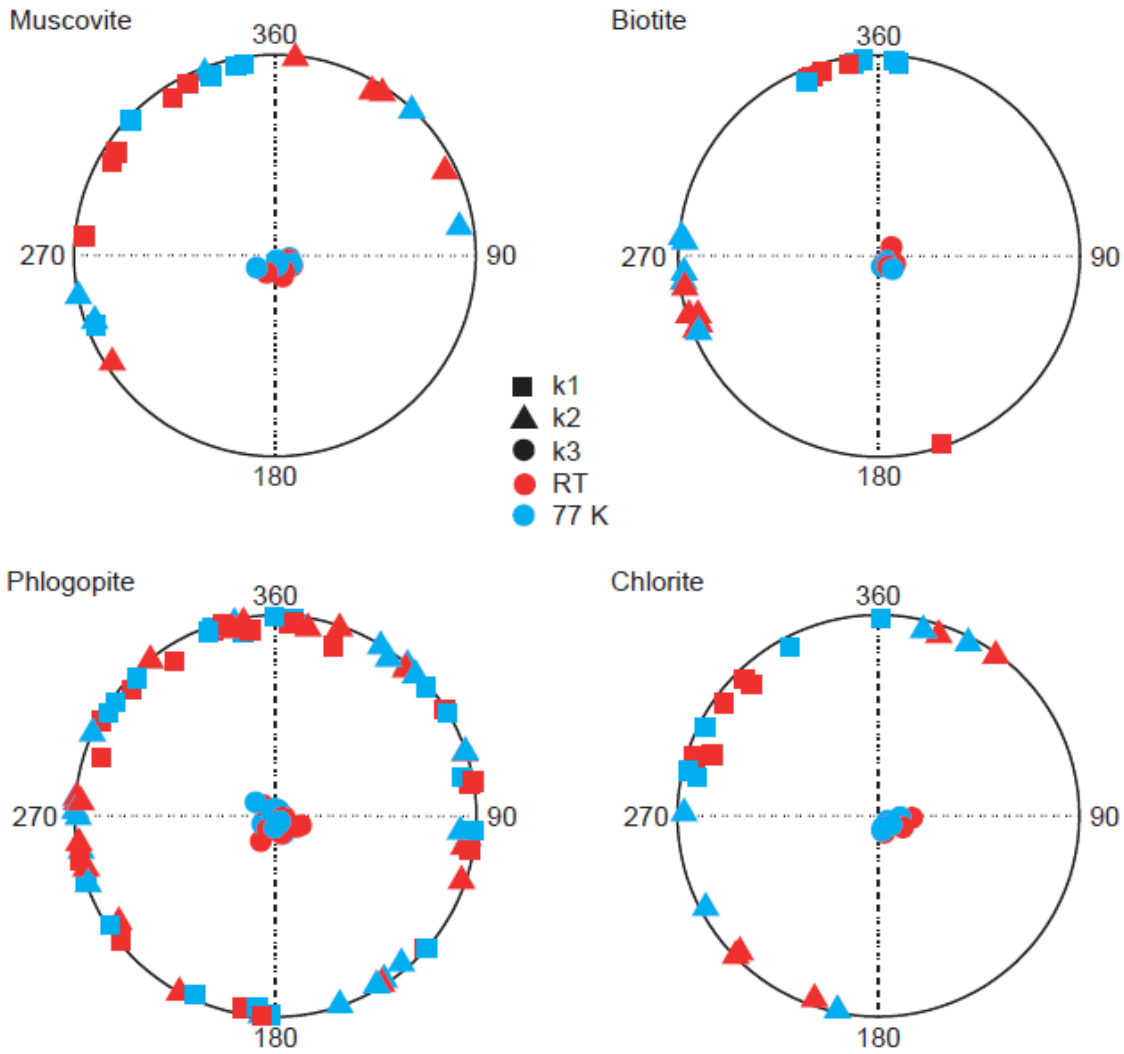

Figure 5: Lower-hemisphere, equal-area stereoplots for the principal susceptibility directions of the paramagnetic component. The vertical direction is perpendicular to the basal plane, whereas the plane of the paper corresponds to the plane of the silicate layers.

Some phlogopite samples from Notre-Dame-du-Laus (e.g. Phl101) show an anisotropy within the basal plane of the mica sheets. In these samples, the anisotropy shape *U* is between 0.2 and 0.7, indicating a triaxial ellipsoid. This triaxiality is present both at room temperature and at 77 K; however, it is stronger at room temperature. Muscovite, even though all samples are oblate, shows slightly lower *U* values than biotite. The increase in degree of anisotropy, as expressed by p_{77} is about 11.2-12.4 for biotite, 6.3-8.7 for phlogopite, and 6.9-8.1 for muscovite.

3.2.3 High-field AMS: Chlorite

Despite the difference in crystallographic structure, the magnetic fabric of chlorite is also controlled by the sheet structure. Torque is dominated by a 2θ term and increases linearly with the square of the applied field with an intercept close to zero. This indicates the dominance of the paramagnetic component. The k_3 axis is normal to the sheet plane, and k_1 and k_2 are distributed within this plane. The magnetic anisotropy is also stronger at 77 K than at room temperature, increasing by a factor between 6.8 and 7.4 (Table 4).

3.3 Low-temperature magnetization curves

All samples show an increase in magnetization or susceptibility with decreasing temperature. At room temperature, the magnetization is 1.1 to 1.7 times weaker when the magnetic field is applied normal to the basal plane than when the field points along a direction within this plane (Figure 6). The samples can be considered to behave as paramagnets at temperatures well above the onset of magnetic ordering. This onset is identified by a reduction of the susceptibility at low temperatures compared to the Curie-Weiss law. Such deviation is observed to occur at higher temperatures when the field is normal to the sheets than when the field is parallel to the sheets. Further, magnetic ordering sets in at lower temperatures in phlogopite and muscovite than in biotite. Curie-Weiss temperatures and g-factors for both directions are summarized in Table 5. Our Curie-Weiss temperatures are consistent with results shown by Beausoleil et al. (1983) for biotite and by Ballet and Coey (1982) for biotite and muscovite.

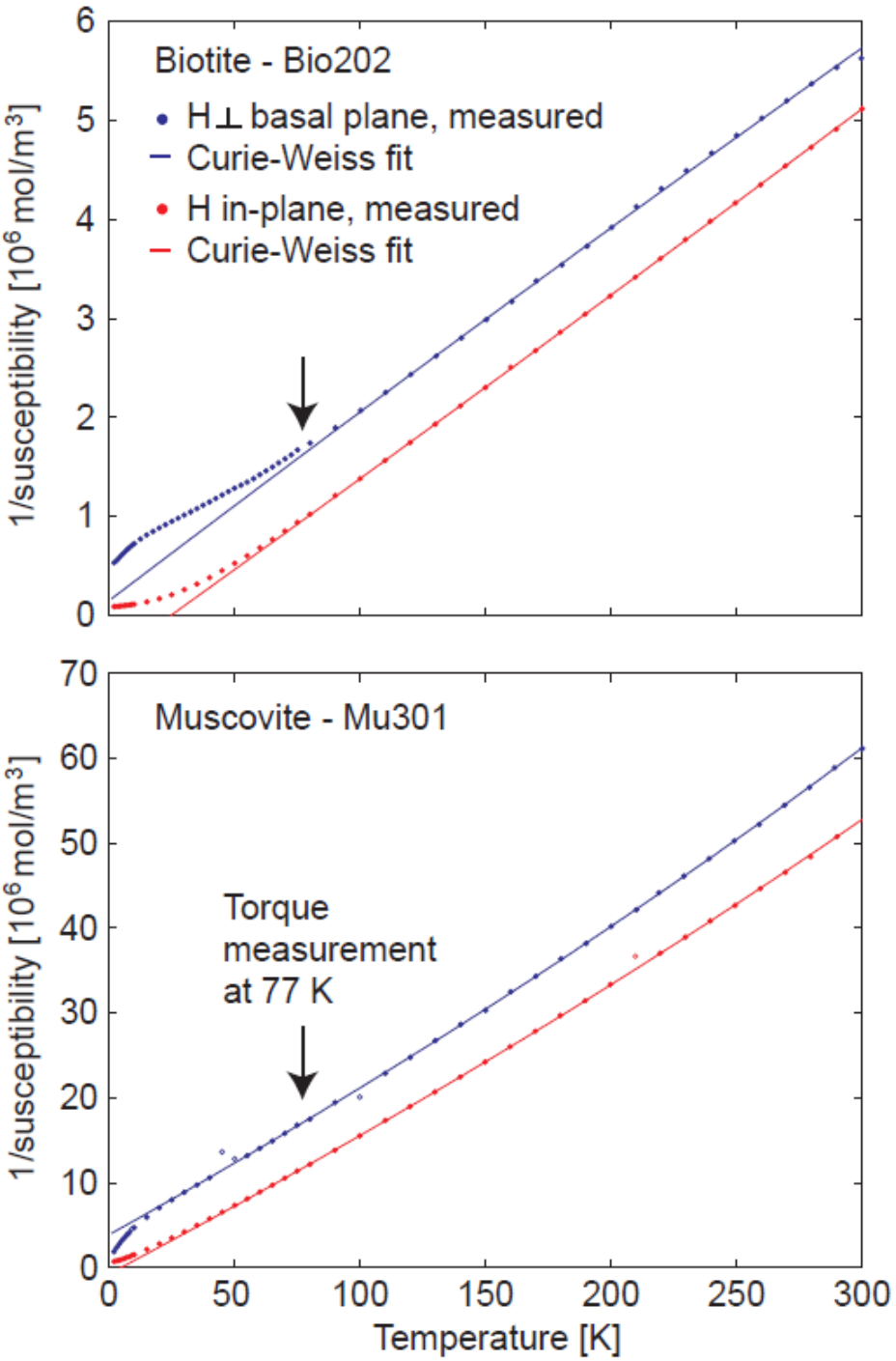

Figure 6: Inverse molar susceptibility as a function of temperature for biotite and muscovite in directions normal and parallel to the basal plane. The susceptibility is smallest normal to the basal plane. In biotite, magnetic ordering sets in above T = 77 K and in muscovite, the ordering temperature is lower.

4. Discussion

Most elements present in common minerals are diamagnetic when in their ionic form. Exceptions are Fe^{2+}, Fe^{3+}, Mn^{2+} and Cr^{3+}. Chromium is normally only present in trace amounts. Therefore, mean susceptibility of a silicate is directly related to its iron and manganese contents (e.g. Vernon, 1961). Bleil and Petersen (1982) calculate mean susceptibility as a function of composition according to the following formula:

$$\chi_g = \mu_0 \frac{L^2}{3RT}(\alpha {p_\alpha}^2 + \beta {p_\beta}^2 + \cdots)$$

where χ_g is mass susceptibility in m^3/kg, $\mu_0 = 4\pi * 10^{-7} \frac{Vs}{Am}$, α, β the concentrations of the elements, $p_\alpha = n_\alpha \mu_B$ with n_α the magnetic moment as a function of μ_B and μ_B the Bohr magneton, *R* the gas constant, *L* Avogadro's number and *T* the temperature. Manganese contents are low in our samples (< 1 wt.% MnO) and therefore the susceptibilities of the samples can be calculated solely on the iron content. We used $5.2\mu_B$ as the effective moment of Fe^{2+} (*cf.* Hoye and O'Reilly, 1972) and and $5.4\mu_B$ for Fe^{3+} (Bleil and Petersen, 1982) for samples whose Fe^{2+}/Fe^{3+} ratio was known. For samples for which we did not have Mössbauer data, we assumed for simplicity that all iron is present as Fe^{2+}. Figure 7 shows the measured susceptibility as a function of the calculated susceptibility. The good correlation ($R^2 \geq 0.98$, excluding Bio101 and Bio104 due to their questionable chemical analysis) and slope close to one indicate that the magnetic properties are dominated by paramagnetic behaviour. This also explains the linear relationship between mean susceptibility and FeO content shown in Figure 3.

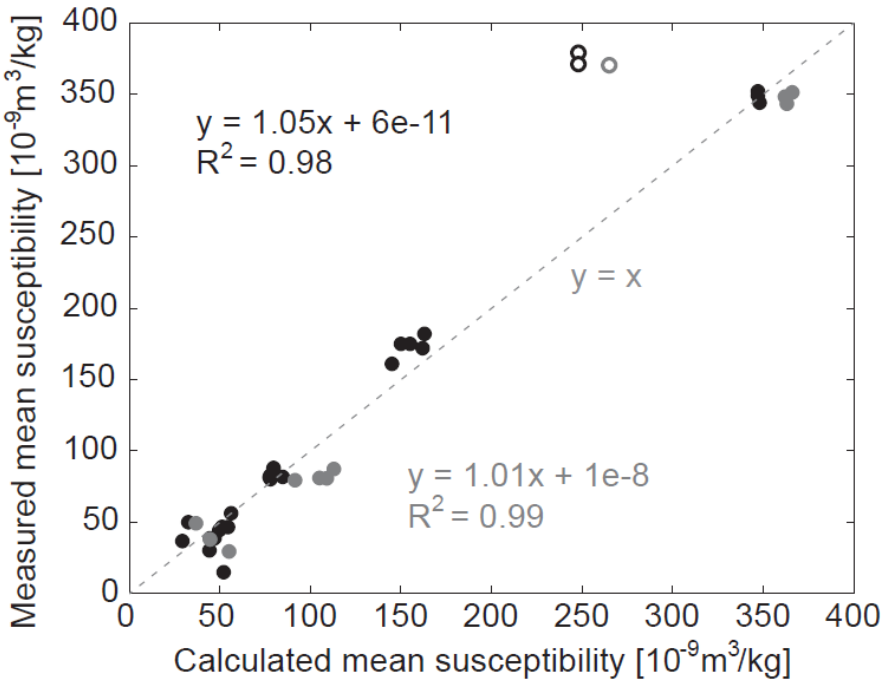

Figure 7: Comparison of measured and calculated mean susceptibility. The calculated susceptibility was determined based on the total Fe content (black) or the corrected FeO and Fe2O3 contents (grey) of the samples. The ideal correlation line with slope one is shown. Only Bio101 and Bio104 fall off this line and are considered as outliers (open symbols).

Mica and chlorite have monoclinic crystal structures and point group 2/m. According to Neumann's principle, a physical property of a crystal must include all the symmetry elements of its point group (Neumann, 1885). Therefore, for a monoclinic crystal, one principal axis of the susceptibility ellipsoid must be parallel to the crystallographic b-axis, which possesses two-fold symmetry. For phyllosilicates in particular it is expected that two principal susceptibility axes lie within the plane of the sheets, while the third principal axis is normal to the sheets, sub-parallel to the c-axis, which is at an angle of 5 – 25° to the normal of the sheets.

Single crystals of muscovite, biotite, phlogopite and chlorite, show that their magnetic anisotropy is dominated by the paramagnetic component with a 2θ term in the two planes perpendicular to the basal plane. The paramagnetic AMS is highly oblate for biotites, muscovites and chlorites. This also applies to most, but not all, of the phlogopite crystals. The

minimum susceptibility is normal to the silicate sheets. If present, only a very small anisotropy can be seen within the sheet plane. Even though the crystal lattice has a monoclinic symmetry, this uniaxial anisotropy can be expected from the phyllosilicate structure. Iron is located within the octahedral sheets, which are separated by the tetrahedral sheets and the interlayer cations. The magnetic interaction within micas and chlorite is characterized by strong ferromagnetic coupling within these octahedral planes and weak antiferromagnetic interactions between them (Ballet and Coey, 1982; Beausoleil et al., 1983). The anisotropy within the sheet plane is slightly larger at low temperature, resulting in a decrease in *U*.

Muscovite generally shows larger anisotropies within the basal plane than biotite, which is in agreement with results of Martín-Hernández and Hirt (2003). Possible reasons are the smaller bulk iron content in muscovite compared to biotite or the different occupancy in the octahedral layer. Muscovite has only 2/3 of its octahedral sites occupied by cations, whereas in biotite all octahedral sites are filled. Muscovite, chlorite and some phlogopite crystals show an anisotropy in their basal plane, which is strongest in the case of phlogopite. This is unexpected, as phlogopite and biotite are members of the same solid solution series. Uyeda et al. (1993) postulated that the triaxiality of the anisotropy may be explained by a diamagnetic signal due to coplanar O_3 units in the sheet silicate structure. These O_3 units are present in all phyllosilicates, but the large paramagnetic AMS due to Fe ions overprints the diamagnetic AMS. However, this is expected to affect the anisotropy of muscovite more strongly in comparison to that of phlogopite, because muscovite contains less iron. Another possibility involves clustering of Fe and Mg ions within the octahedral sheets. Clustering is expected to happen particularly in samples where F^- substitutes for OH^- because iron and F^- tend to avoid each other. Iron clusters in phlogopite due to Fe-F avoidance have been proposed by Sanz and Stone (1979) and Manceau et al. (1990) based on natural magnetic resonance (NMR) and extended X-ray absorption fine structure (EXAFS) studies. Depending on their configuration, these clusters could cause the anisotropy in the basal plane. We tested this latter hypothesis

with STXM, but could not detect any clustering of Fe or Mg with a spatial resolution of 30 – 50 nm. This does not rule out clustering on a smaller scale, however, which could still lead to anisotropy within the plane of the sheet structure.

Martín-Hernández and Hirt (2003) suggested that there may be a correlation between the anisotropy degree and Fe^{2+}/Fe^{3+} ratio, but had too few data to establish a relationship. The anisotropy degree, δk, is higher for biotite than the other minerals both at room temperature and at 77 K, but otherwise there is no clear correlation with either iron content or Fe^{2+}/Fe^{3+} ratio (Figure 8). Moreover, there is also no relationship between degree of anisotropy and the Fe^{2+}/Fe^{3+} ratio at either room temperature or 77 K. Based on theoretical considerations, Ballet and Coey (1982) and Beausoleil et al. (1983), suggested that iron occupies sites of trigonal symmetry and that in this trigonal crystal field, Fe^{3+} behaves isotropically. Fe^{2+}, on the other hand, is affected by the crystal field in a way that it adopts an easy-plane anisotropy, where the hard axis is normal to the octahedral sheets. This could explain the increase of anisotropy with Fe^{2+}/Fe^{3+}.

There is an increase of anisotropy with decreasing temperature as described by p_{77}. Biotite shows the largest value for p_{77}, 12.1 ± 0.5, followed by phlogopite with p_{77} = 8.2 ± 0.6, and chlorite with p_{77} = 7.0 ± 0.3. One muscovite crystal (Mu201) showed a distinct larger increase compared to the other four muscovite crystals. This crystal has the lowest mean susceptibility and lowest Fe content, which may indicate that the diamagnetic contribution to the anisotropy cannot be neglected. A significant diamagnetic component to the anisotropy is not enhanced at 77 K, and therefore leads to a high factor p_{77}. This can be seen for calcite that contains some iron, for which p_{77} = 13.3 for an iron content between 500 to 100,000 ppm (Schmidt et al., 2007a). The paramagnetic contribution to the anisotropy can be isolated from the diamagnetic, by using a mean p_{77} factor of the other four crystals, following the method presented by Schmidt et al. (2007b). This correction leads to a paramagnetic AMS with p_{77} = 7.2, from which we infer that the muscovite increases by 7.4 ± 0.5.

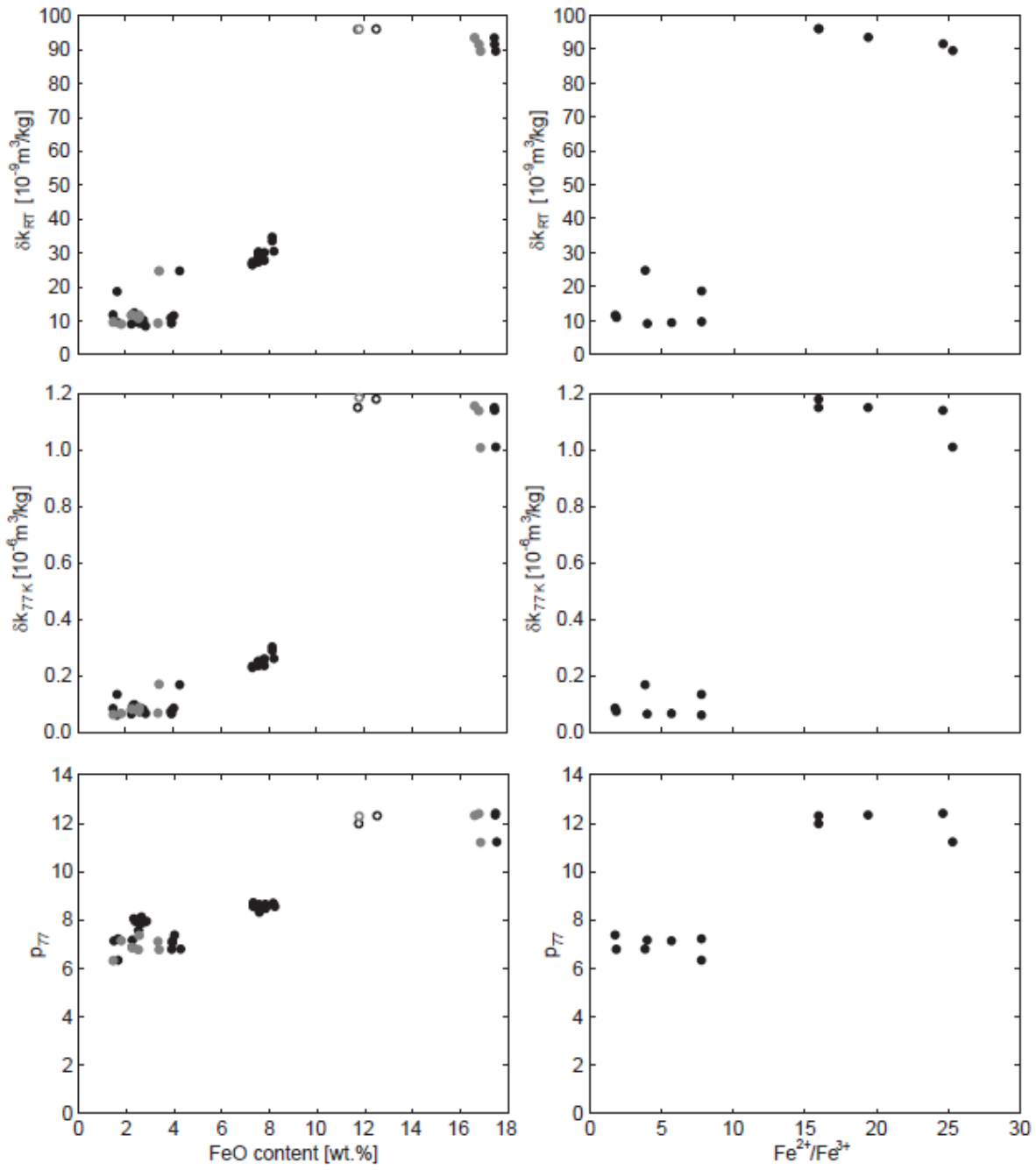

Figure 8:Correlation plots of anisotropy parameters as a function of total iron content (left column, black), Fe2+ content (grey) or Fe2+/Fe3+ (right column), respectively. Note that Fe2+/Fe3+ was only measured on selected samples.

The change in the degree of anisotropy can also be expressed as the ratio between k' determined at 77 K and room temperature, which we have termed p_{77}' in Table 4. The averages are statistically not significantly different from p_{77}, with $p_{77}' = 11.9 \pm 0.5$ for biotite, 8.2 ± 0.6 for phlogopite, 7.2 ± 0.2 for chlorite, and 7.5 ± 0.5 for muscovite.

It is interesting to note that p_{77} is similar to the increase found in siderite, which is on the order of 7.2 ± 0.1. Therefore, several of the common rock-forming minerals show a similar increase in their anisotropy at 77 K. Biotite, however, shows a stronger increase. This is directly related to the onset of magnetic ordering revealed by the low-temperature magnetization curves. The susceptibility of biotite already starts to deviate from paramagnetic behaviour above 77 K when the field is perpendicular to the sheets due to short-range interaction between the magnetic moments of the iron atoms. At the same temperature, biotite still behaves as a paramagnet when the field is parallel to the sheets. Therefore, the anisotropy degree δk at 77 K is larger in biotite compared to a purely paramagnetic crystal with the same composition because antiferromagnetic interactions suppress susceptibility perpendicular to the plane but not in-plane. Phlogopite and muscovite are inside the paramagnetic range in both directions and at both room temperature and 77 K. This difference can be explained by the fact that the Fe concentration is larger in biotite. Here, Fe^{2+} cations are arranged with smaller distances than in the other micas and their interaction is relevant already at 77 K. At room temperature, thermal fluctuations are stronger, hence suppressing magnetic coupling, and biotite behaves as a paramagnet. Similarly, the lower concentration of and larger spacing between Fe sites shift the onset of ferromagnetic (*s.l.*) interactions to lower temperatures in muscovite and phlogopite. This explains why p_{77} is larger in biotite than indicated by the trend of the other micas. This is an important point when measuring AMS at low temperature, because the biotite fabric will be preferentially enhanced with respect to other minerals. Therefore information about p_{77} in various minerals will help in interpreting the magnetic fabric and the responsible minerals at different temperatures.

5. Conclusions

The magnetic anisotropy of biotite, muscovite and chlorite is oblate with the minimum susceptibility normal to the sheet structure, at both room temperature and 77 K. Whereas this is also true for most phlogopites, some phlogopite samples show an additional anisotropy in the basal plane. This anisotropy could be explained by a diamagnetic contribution or the formation of Fe-clusters within the octahedral sheets. The magnetic susceptibilities of mica and chlorite are directly related to the iron content of the minerals, but there is no simple relationship between the iron content and either the degree of anisotropy or p_{77}. There is also no clear correlation between the magnetic anisotropy and the Fe^{2+}/Fe^{3+} ratio. At low temperature, the degree of the anisotropy increases by different amounts depending on the mineral. Biotite with $p_{77} = 12.1 \pm 0.5$ shows the largest increase. For phlogopite, muscovite and chlorite, p_{77} ranges approximately from 7.0 ± 0.3 to 8.2 ± 0.6.

Acknowledgments

S. Bosshard and E. Reusser are thanked for help with the EPMA measurements. The authors acknowledge support by J. Reuteler and E. Müller at the Electron Microscopy Center of ETH Zurich (EMEZ) for sample preparation and imaging. We are grateful to J. Raabe at Swiss Light Source who made the experiments at the PolLux beamline possible. Martin Chadima and an anonymous referee are thanked for their careful reviews that helped to improve this manuscript. This project was funded by the Swiss National Science Foundation under project 129806.

References

Ballet, O., Coey, J.M.D., 1982. Magnetic properties of sheet silicates; 2:1 layer minerals. Physics and Chemistry of Minerals 8, 218-229.

Ballet, O., Coey, J.M.D., Burke, K.J., 1985. Magnetic properties of sheet silicates; 2:1:1 layer minerals. Physics and Chemistry of Minerals 12, 370-378.

Beausoleil, N., Lavallee, P., Yelon, A., Ballet, O., Coey, J.M.D., 1983. Magnetic properties of biotite micas. Journal of Applied Physics 54, 906-915.

Bergmüller, F., Bärlocher, C., Geyer, B., Grieder, M., Heller, F., Zweifel, P., 1994. A torque magnetometer for measurements of the high-field anisotropy of rocks and crystals. Meas Sci Technol 5, 1466-1470.

Bleil, U., Petersen, N., 1982. Magnetische Eigenschaften der Minerale, in: Angenheister, G. (Ed.), Landolt-Börnstein - Numerical Data and Functional Relationships in Science and Technology - Group V: Geophysics and Space Research. Springer, Berlin - Heidelberg - New York.

Borradaile, G., Keeler, W., Alford, C., Sarvas, P., 1987. Anisotropy of magnetic susceptibility of some metamorphic minerals. Physics of the Earth and Planetary Interiors 48, 161-166.

Borradaile, G.J., Lagroix, F., 2000. Thermal enhancement of magnetic fabrics in high grade gneisses. Geophysical Research Letters 27, 2413-2416.

Borradaile, G.J., Werner, T., 1994. Magnetic anisotropy of some phyllosilicates. Tectonophysics 235, 223-248.

Coey, J.M.D., 1988. Magnetic properties of iron in soil iron oxides and clay minerals, in: Stucki, J.W., Goodman, B.A., Schwertmann, U. (Eds.), Iron in Soils and Clay Minerals. Riedl Publ., Dordrecht, pp. 397-466.

Debacker, T.N., Hirt, A.M., Sintubin, M., Robion, P., 2009. Differences between magnetic and mineral fabrics in low-grade, cleaved siliciclastic pelites: A case study from the Anglo-Brabant Deformation Belt (Belgium). Tectonophysics 466, 32-46.

Henry, B., Jordanova, D., Jordanova, N., Derder, M.E.M., Bayou, B., Amenna, M., Dimov, D., 2007. Composite magnetic fabric deciphered using heating treatment. Studia Geophysica Et Geodaetica 51, 293-314.

Hirt, A.M., Lowrie, W., Lüneburg, C., Lebit, H., Engelder, T., 2004. Magnetic and mineral fabric development in the Ordovician Martinsburg Formation in the Central Appalachian Fold and Thrust Belt, Pennsylvania, in: Martín-Hernández, F., Lüneburg, C.M., Aubourg, C., Jackson, M. (Eds.), Magnetic Fabrics: Methods and Applications. Geological Society Special Publications, London, pp. 109-126.

Hoye, G.S., O'Reilly, W., 1972. A magnetic study of the ferro-magnesian olivines (Fe_xMg_{1-x})SiO_4, $0 < x < 1$. Journal of Physics and Chemistry of Solids 33, 1827-1834.

Hrouda, F., Jelinek, V., 1990. Resolution of ferrimagnetic and paramagnetic anisotropies in rocks, using combined low-field and high-field measurements. Geophysical Journal International 103, 75-84.

Ihmlé, P.F., Hirt, A.M., Lowrie, W., Dietrich, D., 1989. Inverse magnetic fabric in deformed limestones of the Morcles Nappe, Switzerland. Geophysical Research Letters 16, 1383-1386.

Jelinek, V., 1981. Characterization of the magnetic fabric of rocks. Tectonophysics, 79, T63-T67.

Jelínek, V., 1984. On a mixed quadratic invariant of the magnetic susceptibility tensor, Journal of Geophysics 56, 58-60.

Kelso, P.R., Tikoff, B., Jackson, M., Sun, W., 2002. A new method for the separation of paramagnetic and ferromagnetic susceptibility anisotropy using low field and high field methods. Geophysical Journal International 151, 345-359.

Lüneburg, C.M., Lampert, S.A., Lebit, H.D., Hirt, A.M., Casey, M., Lowrie, W., 1999. Magnetic anisotropy, rock fabrics and finite strain in deformed sediments of SW Sardinia (Italy). Tectonophysics 307, 51-74.

Manceau, A., Bonnin, D., Stone, W.E.E., Sanz, J., 1990. Distribution of Fe in the octahedral sheet of trioctahedral micas by polarized EXAFS - Comparison with NMR results. Physics and Chemistry of Minerals 17, 363-370.

Martín-Hernández, F., Ferré, E.C., 2007. Separation of paramagnetic and ferrimagnetic anisotropies: A review. Journal of Geophysical Research-Solid Earth 112.

Martín-Hernández, F., Hirt, A.M., 2001. Separation of ferrimagnetic and paramagnetic anisotropies using a high-field torsion magnetometer. Tectonophysics 337, 209-221.

Martín-Hernández, F., Hirt, A.M., 2003. The anisotropy of magnetic susceptibility in biotite, muscovite and chlorite single crystals. Tectonophysics 367, 13-28.

Martín-Hernández, F., Hirt, A.M., 2004. A method for the separation of paramagnetic, ferrimagnetic and haematite magnetic subfabrics using high-field torque magnetometry. Geophysical Journal International 157, 117-127.

Neumann, F.E., 1885. Vorlesungen über die Theorie der Elastizität der festen Körper und des Lichtäthers, in: Meyer, O.E. (Ed.). B.G. Teubner Verlag, Leipzig, Germany.

Pares, J.M., van der Pluijm, B.A., 2002. Phyllosilicate fabric characterization by Low-Temperature Anisotropy of Magnetic Susceptibility (LT-AMS). Geophysical Research Letters 29.

Richter, C., van der Pluijm, B.A., 1994. Separation of paramagnetic and ferrimagnetic susceptibilities using low-temperature magnetic susceptibilities and comparison with high-field methods. Physics of the Earth and Planetary Interiors 82, 113-123.

Rochette, P., 1987. Magnetic susceptibility of the rock matrix related to magnetic fabric studies. Journal of Structural Geology 9, 1015-1020.

Rochette, P., Fillion, G., 1988. Identicication of multicomponent anisotropies in rocks using various field and temperature values in a cryogenic magnetometer. Physics of the Earth and Planetary Interiors 51, 379-386.

Rochette, P., Fillion, G., Mollard, P., Vergne, R., 1983. Rock magnetism - analysis of the magnetic anisotropy in rocks using a cryogenic magnetometer. Comptes Rendus De L Academie Des Sciences Serie II 296, 557-559.

Sanz, J., Stone, W.E.E., 1979. NMR study of micas, II. Distribution of Fe^{2+}, F^-, and OH^- in the octahedral sheet of phlogopites. American Mineralogist 64, 119-126.

Schmidt, V., Hirt, A.M., Hametner, K., Gunther, D., 2007a. Magnetic anisotropy of carbonate minerals at room temperature and 77 K. American Mineralogist 92, 1673-1684.

Schmidt, V., Hirt, A.M., Rosselli, P., Martín-Hernández, F., 2007b. Separation of diamagnetic and paramagnetic anisotropy by high-field, low-temperature torque measurements. Geophysical Journal International 168, 40-47.

Schultz-Krutisch, T., Heller, F., 1985. Measurement of magnetic-susceptibility anisotropy in Buntsandstein deposits from Southern Germany. Journal of Geophysics-Zeitschrift für Geophysik 57, 51-58.

Urrutia-Fucugauchi, J., Tarling, D.H., 1983. Palaeomagnetic properties of Eocambrian sediments in northwestern Scotland: implications for worldwide glaciation in the late Precambrian. Palaeogeography, Palaeoclimatology, Palaeoecology 41, 325-344.

Uyeda, C., Takeuchi, T., Yamagishi, A., Tsuchiyama, A., Yamanaka, T., Date, M., 1993. Diamagnetic anisotropy of sheetsilicates. Physics and Chemistry of Minerals 20, 369-374.

Vernon, R.H., 1961. Magnetic susceptibility as a measure of total iron plus manganese in some ferromagnesian silicate minerals. The American Mineralogist 46, 1141-1153.

Zapletal, K., 1990. Low-field susceptibility anisotropy of some biotite crystals. Physics of the Earth and Planetary Interiors 63, 85-97.

Table 1:

Minerals, sample codes, sample locations, sample masses used for measuring of mean susceptibilities and AMS, and mean susceptibilities. Asterisk indicates that susceptibility was calculated from magnetization curves

Table 2:

Elemental compositions of mineral samples (average and std. deviation of 10 point analyses)

Table 3:

Spectral area of Fe^{2+} and Fe^{3+} components in the Mössbauer spctra and Fe^{2+}/Fe^{3+} ratio of selected samples

Table 4:

Eigenvalues and directions of the paramagnetic component of the high-field AMS determined at 77 K and RT (room temperature) for micas and chlorite. The factors p_{77} and p_{77}‘ describe the increase of the AMS degree with decreasing temperature. %para indicates the contribution of the paramagnetic anisotropy to the total signal.

Table 5:

Curie-Weiss temperatures (θ) and Landé factors (g) for biotite, phlogopite and muscovite when the applied field is perpendicular to the basal plane or in-plane.